Directed Flow of Identified Particles in Au + Au Collisions at $\sqrt{s_{\mathrm{NN}}} = 200$ GeV at RHIC

L. Adamczyk,[9] G. Agakishiev,[19] M. M. Aggarwal,[30] Z. Ahammed,[48] A. V. Alakhverdyants,[19] I. Alekseev,[17] J. Alford,[20] B. D. Anderson,[20] C. D. Anson,[28] D. Arkhipkin,[2] G. S. Averichev,[19] J. Balewski,[24] Banerjee,[48] Z. Barnovska,[12] D. R. Beavis,[2] R. Bellwied,[44] M. J. Betancourt,[24] R. R. Betts,[8] A. Bhasin,[18] A. K. Bhati,[30] H. Bichsel,[50] J. Bielcik,[11] J. Bielcikova,[12] L. C. Bland,[2] I. G. Bordyuzhin,[17] W. Borowski,[41] J. Bouchet,[20] A. V. Brandin,[27] S. G. Brovko,[4] E. Bruna,[52] S. Bueltmann,[29] I. Bunzarov,[19] T. P. Burton,[2] J. Butterworth,[36] X. Z. Cai,[40] H. Caines,[52] M. Calderón de la Barca Sánchez,[4] D. Cebra,[4] R. Cendejas,[5] M. C. Cervantes,[42] P. Chaloupka,[12] S. Chattopadhyay,[48] H. F. Chen,[38] J. H. Chen,[40] J. Y. Chen,[7] L. Chen,[7] J. Cheng,[45] M. Cherney,[10] A. Chikanian,[52] W. Christie,[2] P. Chung,[12] J. Chwastowski,[9] M. J. M. Codrington,[42] R. Corliss,[24] J. G. Cramer,[50] H. J. Crawford,[3] X. Cui,[38] A. Davila Leyva,[43] L. C. De Silva,[44] R. R. Debbe,[2] T. G. Dedovich,[19] J. Deng,[39] R. Derradi de Souza,[6] S. Dhamija,[16] L. Didenko,[2] F. Ding,[4] P. Djawotho,[42] X. Dong,[23] J. L. Drachenberg,[42] J. E. Draper,[4] C. M. Du,[22] L. E. Dunkelberger,[5] J. C. Dunlop,[2] L. G. Efimov,[19] M. Elnimr,[51] J. Engelage,[3] G. Eppley,[36] L. Eun,[23] O. Evdokimov,[8] R. Fatemi,[21] J. Fedorisin,[19] R. G. Fersch,[21] P. Filip,[19] E. Finch,[52] Y. Fisyak,[2] C. A. Gagliardi,[42] D. R. Gangadharan,[28] F. Geurts,[36] S. Gliske,[1] Y. N. Gorbunov,[10] O. G. Grebenyuk,[23] D. Grosnick,[47] S. Gupta,[18] W. Guryn,[2] B. Haag,[4] O. Hajkova,[11] A. Hamed,[42] L-X. Han,[40] J. W. Harris,[52] J. P. Hays-Wehle,[24] S. Heppelmann,[31] A. Hirsch,[33] G. W. Hoffmann,[43] D. J. Hofman,[8] S. Horvat,[52] B. Huang,[38] H. Z. Huang,[5] P. Huck,[7] T. J. Humanic,[28] L. Huo,[42] G. Igo,[5] W. W. Jacobs,[16] C. Jena,[14] J. Joseph,[20] E. G. Judd,[3] S. Kabana,[41] K. Kang,[45] J. Kapitan,[12] K. Kauder,[8] H. W. Ke,[7] D. Keane,[20] A. Kechechyan,[19] A. Kesich,[4] D. Kettler,[50] D. P. Kikola,[33] J. Kiryluk,[23] A. Kisiel,[49] V. Kizka,[19] S. R. Klein,[23] D. D. Koetke,[47] T. Kollegger,[13] J. Konzer,[33] I. Koralt,[29] L. Koroleva,[17] W. Korsch,[21] L. Kotchenda,[27] P. Kravtsov,[27] K. Krueger,[1] L. Kumar,[20] M. A. C. Lamont,[2] J. M. Landgraf,[2] S. LaPointe,[51] J. Lauret,[2] A. Lebedev,[2] R. Lednicky,[19] J. H. Lee,[2] W. Leight,[24] M. J. LeVine,[2] C. Li,[38] L. Li,[43] W. Li,[40] X. Li,[33] X. Li,[39] Y. Li,[45] Z. M. Li,[7] L. M. Lima,[37] M. A. Lisa,[28] F. Liu,[7] T. Ljubicic,[2] W. J. Llope,[36] R. S. Longacre,[2] Y. Lu,[38] X. Luo,[7] A. Luszczak,[9] G. L. Ma,[40] Y. G. Ma,[40] D. P. Mahapatra,[14] R. Majka,[52] O. I. Mall,[4] S. Margetis,[20] C. Markert,[43] H. Masui,[23] H. S. Matis,[23] D. McDonald,[36] T. S. McShane,[10] S. Mioduszewski,[42] M. K. Mitrovski,[2] Y. Mohammed,[42] B. Mohanty,[48] B. Morozov,[17] M. G. Munhoz,[37] M. K. Mustafa,[33] M. Naglis,[23] B. K. Nandi,[15] Md. Nasim,[48] T. K. Nayak,[48] L. V. Nogach,[32] G. Odyniec,[23] A. Ogawa,[2] K. Oh,[34] A. Ohlson,[52] V. Okorokov,[27] E. W. Oldag,[43] R. A. N. Oliveira,[37] D. Olson,[23] M. Pachr,[11] B. S. Page,[16] S. K. Pal,[48] Pan,[5] Y. Pandit,[20] Y. Panebratsev,[19] T. Pawlak,[49] B. Pawlik,[9] H. Pei,[8] C. Perkins,[3] W. Peryt,[49] P. Pile,[2] M. Planinic,[53] J. Pluta,[49] D. Plyku,[29] N. Poljak,[53] J. Porter,[23] A. M. Poskanzer,[23] C. B. Powell,[23] D. Prindle,[50] C. Pruneau,[51] N. K. Pruthi,[30] M. Przybycien,[9] P. R. Pujahari,[15] J. Putschke,[51] H. Qiu,[22] R. Raniwala,[35] S. Raniwala,[35] R. L. Ray,[43] R. Redwine,[24] R. Reed,[4] C. K. Riley,[52] H. G. Ritter,[23] J. B. Roberts,[36] O. V. Rogachevskiy,[19] J. L. Romero,[4] L. Ruan,[2] J. Rusnak,[12] N. R. Sahoo,[48] I. Sakrejda,[23] S. Salur,[23] J. Sandweiss,[52] E. Sangaline,[4] A. Sarkar,[15] J. Schambach,[43] R. P. Scharenberg,[33] A. M. Schmah,[23] N. Schmitz,[25] T. R. Schuster,[13] J. Seele,[24] J. Seger,[10] P. Seyboth,[25] N. Shah,[5] E. Shahaliev,[19] M. Shao,[38] B. Sharma,[30] M. Sharma,[51] S. S. Shi,[7] Q. Y. Shou,[40] E. P. Sichtermann,[23] R. N. Singaraju,[48] M. J. Skoby,[33] N. Smirnov,[52] D. Solanki,[35] P. Sorensen,[2] U. G. deSouza,[37] H. M. Spinka,[1] B. Srivastava,[33] T. D. S. Stanislaus,[47] S. G. Steadman,[24] J. R. Stevens,[16] R. Stock,[13] M. Strikhanov,[27] B. Stringfellow,[33] A. A. P. Suaide,[37] M. C. Suarez,[8] M. Sumbera,[12] X. M. Sun,[23] Y. Sun,[38] Z. Sun,[22] B. Surrow,[24] D. N. Svirida,[17] T. J. M. Symons,[23] A. Szanto de Toledo,[37] J. Takahashi,[6] A. H. Tang,[2] Z. Tang,[38] L. H. Tarini,[51] T. Tarnowsky,[26] D. Thein,[43] J. H. Thomas,[23] J. Tian,[40] A. R. Timmins,[44] D. Tlusty,[12] M. Tokarev,[19] T. A. Trainor,[50] S. Trentalange,[5] R. E. Tribble,[42] P. Tribedy,[48] B. A. Trzeciak,[49] O. D. Tsai,[5] J. Turnau,[9] T. Ullrich,[2] D. G. Underwood,[1] G. Van Buren,[2] G. van Nieuwenhuizen,[24] J. A. Vanfossen, Jr.,[20] R. Varma,[15] G. M. S. Vasconcelos,[6] F. Videbæk,[2] Y. P. Viyogi,[48] S. Vokal,[19] S. A. Voloshin,[51] A. Vossen,[16] M. Wada,[43] F. Wang,[33] G. Wang,[5] H. Wang,[26] J. S. Wang,[22] Q. Wang,[33] X. L. Wang,[38] Y. Wang,[45] G. Webb,[21] J. C. Webb,[2] G. D. Westfall,[26] C. Whitten Jr.,[5] H. Wieman,[23] S. W. Wissink,[16] R. Witt,[46] W. Witzke,[21] Y. F. Wu,[7] Z. Xiao,[45] W. Xie,[33] K. Xin,[36] H. Xu,[22] N. Xu,[23] Q. H. Xu,[39] W. Xu,[5] Y. Xu,[38] Z. Xu,[2] L. Xue,[40] Y. Yang,[22] Y. Yang,[7] P. Yepes,[36] Y. Yi,[33] K. Yip,[2]

I-K. Yoo,[34] M. Zawisza,[49] H. Zbroszczyk,[49] J. B. Zhang,[7] S. Zhang,[40] W. M. Zhang,[20] X. P. Zhang,[45]
Y. Zhang,[38] Z. P. Zhang,[38] F. Zhao,[5] J. Zhao,[40] C. Zhong,[40] X. Zhu,[45] Y. H. Zhu,[40] and Y. Zoulkarneeva[19]

(STAR Collaboration)

[1]*Argonne National Laboratory, Argonne, Illinois 60439, USA*
[2]*Brookhaven National Laboratory, Upton, New York 11973, USA*
[3]*University of California, Berkeley, California 94720, USA*
[4]*University of California, Davis, California 95616, USA*
[5]*University of California, Los Angeles, California 90095, USA*
[6]*Universidade Estadual de Campinas, Sao Paulo, Brazil*
[7]*Central China Normal University (HZNU), Wuhan 430079, China*
[8]*University of Illinois at Chicago, Chicago, Illinois 60607, USA*
[9]*Krakow Universities and Institute*
[10]*Creighton University, Omaha, Nebraska 68178, USA*
[11]*Czech Technical University in Prague, FNSPE, Prague, 115 19, Czech Republic*
[12]*Nuclear Physics Institute AS CR, 250 68 Řež/Prague, Czech Republic*
[13]*University of Frankfurt, Frankfurt, Germany*
[14]*Institute of Physics, Bhubaneswar 751005, India*
[15]*Indian Institute of Technology, Mumbai, India*
[16]*Indiana University, Bloomington, Indiana 47408, USA*
[17]*Alikhanov Institute for Theoretical and Experimental Physics, Moscow, Russia*
[18]*University of Jammu, Jammu 180001, India*
[19]*Joint Institute for Nuclear Research, Dubna, 141 980, Russia*
[20]*Kent State University, Kent, Ohio 44242, USA*
[21]*University of Kentucky, Lexington, Kentucky, 40506-0055, USA*
[22]*Institute of Modern Physics, Lanzhou, China*
[23]*Lawrence Berkeley National Laboratory, Berkeley, California 94720, USA*
[24]*Massachusetts Institute of Technology, Cambridge, MA 02139-4307, USA*
[25]*Max-Planck-Institut für Physik, Munich, Germany*
[26]*Michigan State University, East Lansing, Michigan 48824, USA*
[27]*Moscow Engineering Physics Institute, Moscow Russia*
[28]*Ohio State University, Columbus, Ohio 43210, USA*
[29]*Old Dominion University, Norfolk, VA, 23529, USA*
[30]*Panjab University, Chandigarh 160014, India*
[31]*Pennsylvania State University, University Park, Pennsylvania 16802, USA*
[32]*Institute of High Energy Physics, Protvino, Russia*
[33]*Purdue University, West Lafayette, Indiana 47907, USA*
[34]*Pusan National University, Pusan, Republic of Korea*
[35]*University of Rajasthan, Jaipur 302004, India*
[36]*Rice University, Houston, Texas 77251, USA*
[37]*Universidade de Sao Paulo, Sao Paulo, Brazil*
[38]*University of Science & Technology of China, Hefei 230026, China*
[39]*Shandong University, Jinan, Shandong 250100, China*
[40]*Shanghai Institute of Applied Physics, Shanghai 201800, China*
[41]*SUBATECH, Nantes, France*
[42]*Texas A&M University, College Station, Texas 77843, USA*
[43]*University of Texas, Austin, Texas 78712, USA*
[44]*University of Houston, Houston, TX, 77204, USA*
[45]*Tsinghua University, Beijing 100084, China*
[46]*United States Naval Academy, Annapolis, MD 21402, USA*
[47]*Valparaiso University, Valparaiso, Indiana 46383, USA*
[48]*Variable Energy Cyclotron Centre, Kolkata 700064, India*
[49]*Warsaw University of Technology, Warsaw, Poland*
[50]*University of Washington, Seattle, Washington 98195, USA*
[51]*Wayne State University, Detroit, Michigan 48201, USA*
[52]*Yale University, New Haven, Connecticut 06520, USA*
[53]*University of Zagreb, Zagreb, HR-10002, Croatia*

STAR's measurements of directed flow (v_1) around midrapidity for $\pi^{\pm}$, $K^{\pm}$, K_S^0, p and $\bar{p}$ in Au + Au collisions at $\sqrt{s_{NN}} = 200$ GeV are presented. A negative $v_1(y)$ slope is observed for most of produced particles ($\pi^{\pm}$, $K^{\pm}$, K_S^0 and $\bar{p}$). In 5-30% central collisions a sizable difference is present between the $v_1(y)$ slope of protons and antiprotons, with the former being consistent with zero within errors. The v_1 excitation function is presented. Comparisons to model calculations (RQMD,

UrQMD, AMPT, QGSM with parton recombination, and a hydrodynamics model with a tilted source) are made. For those models which have calculations of v_1 for both pions and protons, none of them can describe $v_1(y)$ for pions and protons simultaneously. The hydrodynamics model with a tilted source as currently implemented cannot explain the centrality dependence of the difference between the $v_1(y)$ slopes of protons and antiprotons.

The BNL Relativistic Heavy Ion Collider (RHIC) was built to study a new form of matter known as the Quark Gluon Plasma (QGP) [1], which existed in the universe shortly after the Big-Bang. At RHIC, two nuclei are collided at near light-speed, and the collision produces thousands of particles due to the significant energy deposited. The collective motion of the produced particles can be characterized [3] by Fourier coefficients,

$$v_n = \langle \cos n(\phi - \psi) \rangle \tag{1}$$

where n denotes the harmonic, ϕ and ψ denote the azimuthal angle of an outgoing particle and reaction plane, respectively. The reaction plane is defined by the collision axis and the line connecting the centers of two nuclei. Thus far, five of these coefficients have been measured and found to be non-zero at RHIC [2]. They are directed flow v_1, elliptic flow v_2, triangular flow v_3, the 4th order harmonic flow v_4 and the 6th order harmonic flow v_6. This paper will focus on the directed flow, the first Fourier coefficient.

Directed flow describes the sideward motion of produced particles in ultra-relativistic nuclear collisions. It is believed to be generated during the nuclear passage time before the thermalization happens, thus it carries early information from the collision [4–7]. The shape of directed flow at midrapidity may be modified by the collective expansion and reveal a signature of a possible phase transition from normal nuclear matter to a QGP [8–10]. It is argued that directed flow, as an odd function of rapidity (y), may exhibit a small slope (flatness) at midrapidity due to a strong expansion of the fireball being tilted away from the collision axis. Such tilted expansion gives rise to anti-flow [8] or a 3rd flow [9] component (not the third flow harmonic). The anti-flow (or the 3rd flow component) is perpendicular to the source surface, and is in the opposite direction to the bouncing-off motion of nucleons. If the tilted expansion is strong enough, it can even overcome the bouncing-off motion and results in a negative $v_1(y)$ slope at midrapidity, potentially producing a wiggle-like structure in $v_1(y)$. Note that although calculations [8, 9] for both anti-flow and 3rd flow component are made for collisions at SPS energies where the first order phase transition to a QGP is believed to be the most relevant [10], the direct cause of the negative slope is the strong, tilted

expansion, which is also important at RHIC's top energies. Indeed hydrodynamic calculations [11] for Au + Au collisions at $\sqrt{s_{NN}} = 200$ GeV with a tilted source as the initial condition can give a similar negative $v_1(y)$ slope as that found in data. A wiggle structure is also seen in the Relativistic Quantum Molecular Dynamics (RQMD) model [12], and it is attributed to baryon stopping together with a positive space-momentum correlation. In this picture, no phase transition is needed, and pions and nucleons flow in opposite directions. To distinguish between baryon stopping and anti-flow, it is desirable to measure the $v_1(y)$ for identified particles and compare the sign of their slopes at midrapidity. In particular, the observation of a centrality dependence of proton $v_1(y)$ may reveal the character of a possible first order phase transition [10]. It is expected that in very peripheral collisions the bouncing-off motion dominates over the entire rapidity range, and protons at midrapidity flow in the same direction as spectators. In mid-central collisions, if there is a phase transition, the proton $v_1(y)$ slope at midrapidity may change sign and become negative. Eventually the slope diminishes in central collisions due to the symmetry of the collisions.

At low energies, the E895 collaboration has shown that K_S^0 has a negative $v_1(y)$ slope around midrapidity [13], while Λ and protons have positive slopes [14]. This is explained by a repulsive kaon-nucleon potential and an attractive Λ-nucleon potential. The NA49 collaboration [15] has measured v_1 for pions and protons, and a negative $v_1(y)$ slope is observed by the standard event plane method. The three-particle correlation method $v_1\{3\}$ [16], which is believed to be less sensitive to non-flow effects, gives a negative slope too, but with a larger statistical error. The non-flow effects are correlations among particles that are not related to the reaction plane, including the quantum Hanbury Brown-Twiss correlation [17], resonance decays [18] and so on. At top RHIC energies, v_1 has been studied mostly for charged particles by both the STAR and the PHOBOS collaborations [19–22]. It is found that v_1 in the forward region follows the limiting fragmentation hypothesis [23], and v_1 as a function of pseudorapidity (η) depends only on the incident energy, but not on the size of the colliding system at a given centrality. Such system size independence of v_1 can be explained by the hydrodynamic calculation with

a tilted initial condition [11]. The systematic study of v_1 for identified particles at RHIC did not begin until recently because it is more challenging for two reasons: 1) v_1 for some identified particles (for example, protons) is much smaller than that of all charged particles, 2) more statistics are needed to determine v_1 for identified particles other than pions.

54 million events from Au + Au collisions at $\sqrt{s_{NN}} = 200$ GeV have been used in this study, all taken by a minimum-bias trigger with the STAR detector during RHIC's seventh run in year 2007. The main trigger detector used is the Vertex Position Detector (VPD) [24]. The centrality definition of an event was based on the number of charged tracks in the Time Projection Chamber (TPC) [25] with track quality cuts: $|\eta| < 0.5$, a Distance of Closest Approach (DCA) to the vertex less than 3 cm, and 10 or more fit points. In the analysis, events are required to have the vertex z within 30 cm from the center of the TPC, and additional weight is assigned to each event in the analysis accounting for the non-uniform VPD trigger efficiency in the vertex z direction for different centrality classes. The event plane angle is determined from the sideward deflection of spectator neutrons measured by STAR's Shower Maximum Detector inside the Zero Degree Calorimeters (ZDC-SMDs). Such sideward deflection of spectator neutrons is expected to happen in the reaction plane rather than participant plane, since the ZDC-SMDs are located close to beam rapidity. Being 6 units in η away from midrapidity, ZDC-SMDs also allow a measurement of v_1 with minimal contribution from non-flow correlations. The description of measuring v_1 using the ZDC-SMDs event plane can be found in [21]. Particle Identification (PID) of charged particles is achieved by measuring ionization energy loss (dE/dx) inside STAR's TPC, together with the measurement of the momentum (p) via TPC tracking. Track quality cuts are the same as used in [26]. In addition, the transverse momentum p_T for protons is required to be larger than 400 MeV/c, and DCA is required to be less than 1 cm in order to avoid including background protons which are from knock-out/nuclear interactions of pions with inner detector material. The same cuts are applied to antiprotons as well to ensure a fair comparison with protons. The high-end of the p_T cut is 1 GeV/c where protons and pions have the same energy loss in the TPC and thus become indistinguishable. For pions and kaons, p_T range is 0.15 - 0.75 GeV/c and 0.2 - 0.6 GeV/c, respectively. $K_S^0(\to \pi^+\pi^-)$ are topologically reconstructed by their charged daughter tracks inside TPC [27].

Results presented in the following figures contain only statistical errors. Results for pions, protons and antiprotons are not corrected for the feeddown from weak decay particles. The major systematic error in
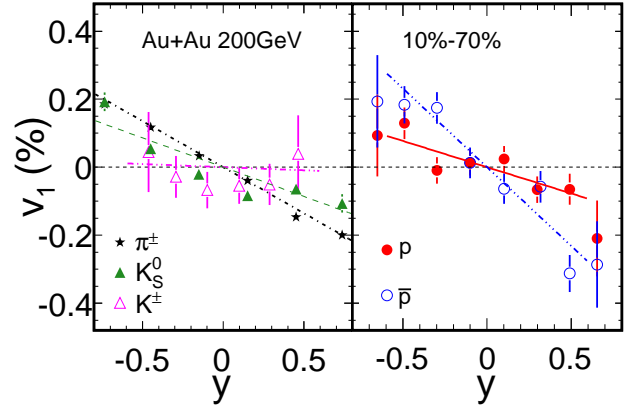

FIG. 1: v_1 for $\pi^\pm$, $K^\pm$, K_S^0 (left panel), p and $\bar{p}$ (right panel) as a function of rapidity for 10-70% Au + Au collisions at $\sqrt{s_{NN}} = 200$ GeV. The lines present the linear fit to the $\pi^\pm$, $K^\pm$, K_S^0, p and $\bar{p}$'s $v_1(y)$ respectively. Data points around $y = 0.29$ are slightly shifted horizontally to avoid overlapping.

determining the slope of $v_1(y)$ for identified particles is from the particle misidentification, which was evaluated by varying the dE/dx cut. Another systematic error comes from the non-uniform p_T acceptance, as $v_1(y)$ is obtained by integrating v_1 over the p_T acceptance which itself depends on the rapidity. This effect is non-negligible for protons and antiprotons at large rapidity. It is estimated by taking the difference between slopes fitted with points integrated with p_T acceptance at midrapidity and at large rapidity. In addition, some of the observed protons have originated from interactions between the produced particles and the detector material, and such effect has also been taken into consideration. The total systematic uncertainty is obtained by adding uncertainties mentioned above in quadrature. There are also common systematic errors that should be applied to all particles: the uncertainty due to the first order event plane determination, which was estimated to be $\sim 10\%$ (relative error) [21], and the uncertainty due to centrality selection, which was estimated to be $\sim 4\%$ (relative error) by comparing our charged $v_1(\eta)$ slope to that from the RHIC run in 2004. Other systematic errors have been evaluated to be negligible.

In Fig. 1, $v_1(y)$ of $\pi^\pm$, $K^\pm$, K_S^0, p, and $\bar{p}$ are presented for centrality 10-70%. Following convention, the sign of spectator v_1 in the forward region is chosen to be positive, to which the measured sign of v_1 for particles of interest is only relative. Fitting with a linear function, the slopes are $-0.15 \pm 0.05(\text{stat}) \pm 0.08(\text{sys})(\%)$ for the protons, $-0.46 \pm 0.06(\text{stat}) \pm 0.04(\text{sys})(\%)$ for the antiprotons, $-0.27 \pm 0.01(\text{stat}) \pm 0.01(\text{sys})(\%)$ for the pi-
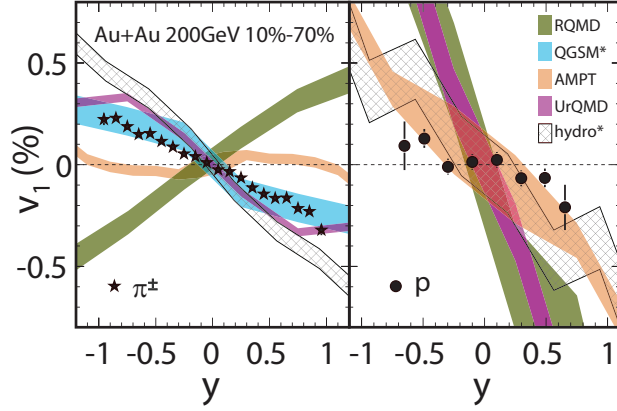
FIG. 2: Model calculations of pion (left panel) and proton (right panel) $v_1(y)$ for 10-70% Au + Au collisions at $\sqrt{s_{NN}} = 200$ GeV. QGSM* model presents the basic Quark-Gluon String model with parton recombination [30]. Hydro* model presents the hydrodynamic expansion from a tilted source [11].

FIG. 3: Charged pions (solid stars), protons (solid circles) and antiprotons (solid squares) $v_1(y)$ slope (dv_1/dy) at midrapidity as a function of centrality for Au + Au collisions at $\sqrt{s_{NN}} = 200$ GeV.

ons, -0.02 ± 0.11(stat)± 0.04(sys)(%) for the kaons and -0.17 ± 0.02(stat)± 0.04(sys)(%) for the K_S^0. The relative 10% common systematic error for all particles is not listed here. The $v_1(y)$ slope for the produced particle types ($\pi^\pm$, $K^\pm$, K_S^0 and $\bar{p}$) are mostly found to be negative at mid-rapidity, which is consistent with the anti-flow picture. In particular, kaons are less sensitive to shadowing effects due to the small kaon-nucleon cross section, yet it shows a negative slope. This is again consistent with the anti-flow picture. Interestingly, $v_1(y)$ for protons exhibits a clearly flatter shape than that for antiprotons. While mass may contribute to the difference in slope between pions and protons/antiprotons, it cannot explain the difference in slope observed for antiprotons and protons. Indeed, the observed v_1 for protons is a convolution of directed flow of produced protons with that of transported protons (from the original projectile and target nuclei), so the flatness of inclusive proton $v_1(y)$ around midrapidity could be explained by the negative flow of produced protons being compensated by the positive flow of protons transported from spectator rapidity, as a feature expected in the anti-flow picture.

In Fig. 2, pion and proton $v_1(y)$ are plotted together with five model calculations, namely, RQMD [12], UrQMD [28], AMPT [29], QGSM with parton recombination [30], and slopes from an ideal hydrodynamic calculation with a tilted source [11]. The model calculations are performed in the same p_T acceptance and centrality as the data. The RQMD and AMPT model calculations predict the wrong sign and wrong magnitude of pion $v_1(y)$, respectively, while the RQMD and the UrQMD predict the
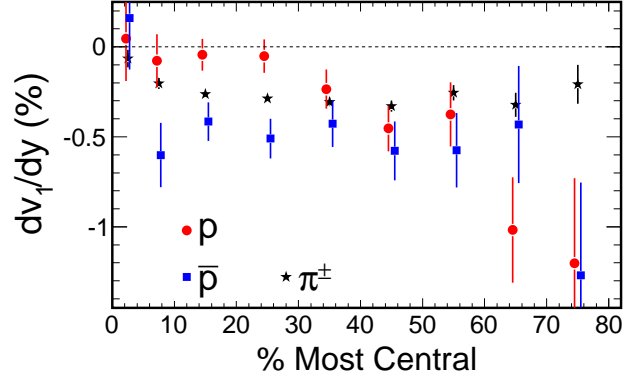
wrong magnitude of proton $v_1(y)$. For models other than QGSM which has the calculation only for pions, none of them can describe $v_1(y)$ for pions and protons simultaneously.

In Fig. 3, the slope of $v_1(y)$ at midrapidity is presented as a function of centrality for protons, antiprotons, and charged pions. In general, the magnitude of the $v_1(y)$ slope converge to zero as expected for most central collisions. Proton and antiproton $v_1(y)$ slope are more or less consistent in 30-80% centrality range but, diverge in 5-30% centrality. In addition, two observations are noteworthy: i) the hydrodynamic model with tilted source (which is a characteristic of anti-flow) as currently implemented does not predict the difference in $v_1(y)$ between particle species [31]. ii) If the difference between v_1 of protons and antiprotons is caused by anti-flow alone, then such difference is expected to be accompanied by strongly negative v_1 slopes. In data, the large difference between proton and antiproton v_1 slopes is seen in the 5-30% centrality range, while strongly negative v_1 slopes are found for protons, antiprotons and charged pions in a different centrality range (30-80%). Both observations suggest that additional mechanisms than that assumed in [11, 31] are needed to explain the centrality dependence of the difference between the $v_1(y)$ slopes of protons and antiprotons.

The excitation function of proton $v_1(y')$ slope F ($= dv_1/dy'$ at midrapidity) is presented in Fig 4. Values for F are extracted via a polynomial fit of the form $Fy' + Cy'^3$, where $y' = y/y_{beam}$ for which spectators are normalized at ± 1. The proton $v_1(y')$ slope decreases rapidly with increasing energy, reaching zero around $\sqrt{s_{NN}} = 9$ GeV. Its sign changes to negative as shown by the data point at $\sqrt{s_{NN}} = 17$ GeV, measured by the NA49 experiment [15]. A similar trend has been observed at low energies with a
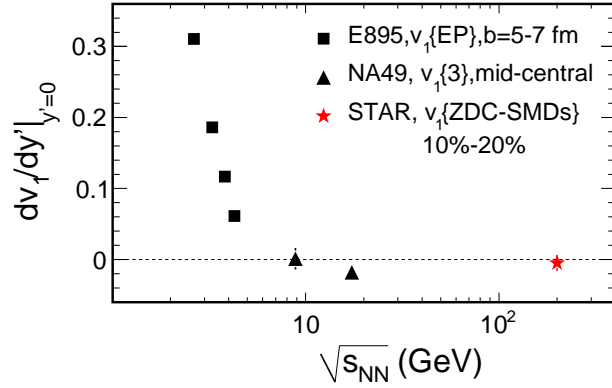
FIG. 4: Proton $v_1(y^{'})$ slope $(dv_1/dy^{'})$ at midrapidity as a function of center of mass collision energy, where $y^{'} = y/y_{beam}$.

slightly different quantity $d\langle p_x \rangle/dy'$ [32, 33]. The energy dependence of $v_1(y')$ slope for protons is driven by two factors, i) the increase in the number of produced protons over transported protons with increasing energy, and ii) the v_1 of both produced and transported protons at different energies. The negative $v_1(y')$ slope for protons around midrapidity at SPS energies cannot be explained by transport model calculations like UrQMD [34] and AMPT [29], but is predicted by hydro calculations [8, 9]. The present data indicate that the proton v_1 slope remains close to zero at $\sqrt{s_{NN}} = 200$ GeV as observed at $\sqrt{s_{NN}} = 9$ GeV and $\sqrt{s_{NN}} = 17$ GeV heavy ion collisions. Our measurement offers a unique check of the validity of a tilted expansion at RHIC top energy.

In summary, STAR's measurements of directed flow of pions, kaons, protons, and antiprotons for Au + Au collisions at $\sqrt{s_{NN}} = 200$ GeV are presented. In the range of 10-70% central collisions, $v_1(y)$ slopes of pions, kaons (K_S^0), and antiprotons

are found to be mostly negative at mid-rapidity. In 5-30% central collisions a sizable difference is present between the $v_1(y)$ slope of protons and antiprotons, with the former being consistent with zero within errors. Comparison to models (RQMD, UrQMD, AMPT, QGSM with parton recombination, and hydrodynamics with a tilted source) is made. Putting aside the QGSM model which has the calculation only for pions, none of the other models explored can describe $v_1(y)$ for pions and protons simultaneously. Additional mechanisms than that assumed in the hydrodynamic model with a tilted source [11, 31] are needed to explain the centrality dependence of the difference between the $v_1(y)$ slopes of protons and antiprotons. Our measurement indicates that the proton's $v_1(y)$ slope remains close to zero for Au + Au collisions at $\sqrt{s_{NN}} = 200$ GeV. These new measurements on the particle species and centrality dependence of $v_1(y)$ provides a check for the validity of a tilted expansion at RHIC top energy.

[1] BRAHMS, PHENIX, PHOBOS, and STAR Collaboration, *Nucl. Phys. A* **757** Issues 1-2 (2005).
[2] S. Voloshin, A. Poskanzer and R. Snellings, Volume 23, In *Relativistic Heavy Ion Physics*, Published by Springer-Verlag. Edited by R. Stock. DOI: 10.1007/978-3-642-01539-7. arXiv:0809.2949
[3] A. M. Poskanzer and S. A. Voloshin, *Phys. Rev. C* **58**, 1671 (1998).
[4] E. Schnedermann and U. Heinz, *Phys. Rev. Lett.* **69**, 2908 (1992).
[5] D. E. Kahana, D. Keane, Y. Pang, T. Schlagel and S. Wang, *Phys. Rev. Lett.* **74**, 4404 (1995).
[6] J. Barrette *et al.* (E877 Collaboration), *Phys. Rev. Lett.* **73**, 2532 (1994).
[7] I. G. Bearden *et al.* (NA44 Collaboration), *Phys. Rev. Lett.* **78**, 2080 (1997).
[8] J. Brachmann *et al.*, *Phys. Rev. C* **61**, 024909 (2000).
[9] L. P. Csernai and D. Röhrich, *Phys. Lett. B* **458**, 454 (1999).
[10] H. Stöcker, *Nucl. Phys. A* **750**, 121 (2005).
[11] P. Bożek and I. Wyskiel, *Phys. Rev. C* **81**, 054902 (2010).
[12] R. J. M. Snellings, H. Sorge, S. A. Voloshin, F. Q. Wang and N. Xu, *Phys. Rev. Lett* **84**, 2803 (2000).
[13] P. Chung *et al.* (E895 Collaboration), *Phys. Rev. Lett.* **85**, 940 (2000).
[14] P. Chung *et al.* (E895 Collaboration), *Phys. Rev.*

Lett. **86**, 2533 (2001).

[15] C. Alt *et al.* (NA49 Collaboration), *Phys. Rev. C* **68**, 034903 (2003).

[16] N. Borghini, P. M. Dinh and J.-Y. Ollitrault, *Phys. Rev. C* **66**, 014905 (2002).

[17] P. M. Dinh, N. Borghini and J.-Y. Ollitrault, *Phys. Lett. B* **477**, 51 (2000).

[18] N. Borghini, P. M. Dinh and J.-Y. Ollitrault, *Phys. Rev. C* **62**, 034902 (2000).

[19] J. Adams *et al.* (STAR Collaboration), *Phys. Rev. Lett.* **92**, 062301 (2004).

[20] B. B. Back *et al.* (PHOBOS Collaboration), *Phys. Rev. Lett* **97**, 012301 (2006).

[21] J. Adams *et al.* (STAR Collaboration), *Phys. Rev. C* **73**, 034903 (2006).

[22] B. I. Abelev *et al.* (STAR Collaboration), *Phys. Rev. Lett.* **101**, 252301 (2008).

[23] J. Benecke *et al.*, *Phys. Rev.* **188**, 2159 (1969).

[24] W. J. Llope *et al.*, *Nucl. Instrum. Methods A* **522**, 252 (2004).

[25] M. Anderson *et al.*, *Nucl. Instrum. Method. A* **499**, 659 (2003).

[26] J. Adams *et al.* (STAR Collaboration), *Phys. Rev. C* **72**, 014904 (2005).

[27] C. Adler *et al.* (STAR Collaboration), *Phys. Rev. Lett.* **89**, 132301 (2002); J. Adams *et al.* (STAR Collaboration), *Phys. Rev. Lett.* **92**, 052302 (2004).

[28] M. Bleicher and H. Stöcker, *Phys. Lett. B* **526**, 309 (2002).

[29] J. Y. Chen *et al.*, *Phys. Rev. C* **81**, 014904 (2010).

[30] J. Bleibel, G. Burau, A. Faessler and C. Fuchs, *Phys. Rev. C* **76**, 024912 (2007).

[31] P. Bożek, private communication, 2010.

[32] H. Liu *et al.* (E895 Collaboration), *Phys. Rev. Lett.* **84**, 5488 (2000).

[33] J. Barrette *et al.* (E877 Collaboration), *Phys. Rev. C* **56**, 3254 (1997); *Phys. Rev. C* **55**, 1420 (1997).

[34] H. Petersen, Q. Li, X. Zhu and M. Bleicher, *Phys. Rev. C* **74**, 064908 (2006).